J Polym Res (2015) 22: 77
DOI 10.1007/s10965-015-0729-z

ORIGINAL PAPER

Poly(amide-imide) bearing imidazole groups/sulfonated polyimide blends for low humidity and medium temperature proton exchange membranes

Elaheh Kowsari[1] · **Vahid Ansari**[1] · **Abbas Moradi**[2] · **Alireza Zare**[1] · **Mehrzad Mortezaei**[2,3]

Received: 7 January 2015 / Accepted: 6 April 2015 / Published online: 15 April 2015

Abstract A poly(amide-imide) (PAI) bearing imidazole groups on the polymer chain was synthesized via direct polycondensation of a synthesized diacid-diimide and 4,4′-(1,4-Phenylenediisopropylidene) bisaniline (PDBA). Diacide-diimide was synthesized by the condensation of an amino acid compound, (S)-(+)-Histidine hydrochloride monohydrate and 3,3′,4,4′-Benzophenone tetracarboxylic dianhydride (BTDA). On the other hand, a sulfonated polyimide (SPI) was also synthesized by the solution imidization of sulfonated, (4,4-diaminostilbene-2,2-disulfonic acid) (DSDSA) and non-sulfonated, 4,4′-(1,4-Phenylenediisopropylidene) bisaniline (PDBA) diamines in reaction with a six-membered naphthalene base dianhydride, 1,4,5,8-Naphthalenetetracarboxylic dianhydride (NTDA). A strong and flexible SPI membrane with good uniformity and proper thermal and mechanical properties was achieved. The SPI was then blended with different amounts of PAI and doped with phosphoric acid (PA), in order to investigate the blending influence of PAI in PA-doped blend membranes compared to the pure SPI membrane. It was found that a proper amount of PAI could effectively improve the water uptake, IEC and proton conductivity of the PA doped SPI/PAI membranes. Nevertheless the excess PAI negatively affected the membrane properties. The pure SPI with an IEC of 1.76 meq.g^{-1} showed a proton conductivity of 29.4 mS cm^{-1} at 120 °C, while PA doped SPI/PAI-10 % (*w/w*) as the most optimal PAI containing sample, with an IEC of 2.23, showed a proton conductivity of 69.7 mS cm^{-1} at 140 °C. The proton conductivity measurements were performed at 40 % relative humidity.

Keywords Poly(amide-imide) · Imidazole · Sulfonated polyimide · Proton exchange membrane · Phosphoric acid

✉ Elaheh Kowsari
kowsarie@aut.ac.ir

[1] Department of Chemistry, Amirkabir University of Technology, Tehran, Iran

[2] Islamic Azad University, Tehran South Branch, Tehran, Iran

[3] Polymer Engineering Group, Composite Science and Technology Research Center, Tehran, Iran

Introduction

Polymer electrolyte membranes are currently under active development for electric vehicles, residential power sources, and portable devices and have attracted much attention due to their important application in fuel cell systems. In the past few decades, various kinds of sulfonated aromatic polymers such as sulfonated poly(arylene ether)s like poly(ether ether ketone) PEEK and poly(sulfone), polybenzimidazole (PBI) and sulfonated polyimide (SPI) have been introduced for the development of high performing polymer electrolyte membranes as cheaper alternatives to the perfluorosulfonic acid (PFSA) membranes, Nafion, as the most common polymer for PEMFC application. Nafion has excellent chemical stability, mechanical strength, flexibility, durability and high conductivity in hydrated state, but besides the high cost problem, they have a number of disadvantages such as high methanol permeability and poor performance at temperatures above 80 °C due to the loss of water, which limit their wider application in higher temperatures and low humidity states [1–5]. Recently great spectra of researches have been focused on the development of membranes that operate at medium-high temperatures (100–200 °C) and low relative humidity states [6–12]. Fuel cells operating at high temperatures offer many advantages, including simpler water management, higher CO tolerance and faster electrode kinetics [8, 13–15].

Sulfonated six-membered ring polyimides, as membranes possessing high thermal stability, mechanical strength and chemical resistance and also low cost, have been identified as one of the promising candidates for medium-high temperature proton conductive membranes. Many SPI membranes with various chemical structures have been reported in recent researches. SPI membranes rely on water as a proton carrier, so water uptake and degree of sulfonation are important issues. A high degree of sulfonation can provide sulfonated aromatic hydrocarbon polymers with high proton conductivity, but the high degree of sulfonation might decrease their mechanical strength and also make them highly swell-able in water or even soluble in aqueous methanol solution. Sulfonation degrees can be controlled by copolymerization with non-sulfonated diamine monomers. The introduction of non-sulfonated diamines decreases the proton conductivity, but can improve the water stability and mechanical properties of membrane [16–23]. During the past decade, many types of membranes such as inorganic polymer composites, non-fluorinated hydrocarbon polymers and anhydrous proton conducting polymers have been developed for improving the performance of the membranes above 100 °C at lower relative humidity [2, 24–27]. Recently, various kinds of aromatic polybenzimidazoles (PBIs) and their blend membranes also have received considerable attention for high temperature and low humidifying polymer electrolyte membrane fuel cells [28–31]. It has been found that phosphoric acid doped sulfonated PBI membranes have shown higher proton conductivities than the corresponding phosphoric acid doped non-sulfonated PBI membranes [32, 33]. Phosphoric acid, as a thermally stable triprotic amphoteric acid and excellent proton conductivity with low vapor pressure at elevated temperature, is a good proton solvent for membranes operating in high temperature ranges. Phosphoric acid can also be doped into membranes of thermally stable polymers such as polyimide and polybenzimidazole. The proton conductivity of PI/H_3PO_4 blends is still lower than that of polybenzimidazole (PBI)/H_3PO_4 blends due to the weaker Lewis basicity of PI and lower H_3PO_4 doping ability [34–36]. So it can be expected that introducing stronger basic groups into the PI in the PI/H_3PO_4 membranes would give us higher conductivities, and also PA doped sulfonated polyimide could show higher conductivities than that of PA doped non-sulfonated polyimide. It is indicated that heteroaromatic polymers containing groups such as imidazole, pyrazole, and triazole are capable of showing high conductivity in low humidity states at higher temperatures. The basic nitrogen groups of these compounds as a strong proton acceptor with respect to the strong acidic groups, can increase the proton conductivity of membranes when be doped with phosphoric acid, through the formation of acid-base complexes, which behave as durable acid container sites [37–39]. These results stimulated us to investigate the influence of blending a synthesized imidazole containing polymer on the proton conductivity of SPI blend membranes. Polymer blending is an adjustable technique for producing new materials with improved physical and chemical properties.

In the present work, we report the synthesis and characterization of a poly(amide-imide), containing imidazole groups, which is capable of being doped with phosphoric acid, to be blended with a synthesized sulfonated polyimide. The sulfonated polyimide with 50 % molar ratio of sulfonated diamine is expected to have good thermal and mechanical properties and appropriate proton conductivity. In addition, blending of PAI with SPI and sequenced doping of membranes with phosphoric acid is supposed to increase the proton conductivity of the membranes, especially at higher temperatures. Achieving to the optimum amounts of blended PAI with SPI is of great importance in this work. It is expected that Phosphoric acid doped SPI/PAI membranes could overcome the water loss problems of SPI membranes at high temperatures. Proton conductivity of the membranes was tested from room temperature to 140 °C, at ambient humidity (40 % RH) and without further humidification. Thermal and mechanical properties, morphology, water uptake and ion exchange capacity (IEC) of the samples are also discussed.

Experimental

Materials

4,4-diaminostilbene-2,2-disulfonic acid (DSDSA), 1,4,5,8-Naphthalenetetracarboxylic dianhydride (NTDA), 3,3′,4,4′-Benzophenone tetracarboxylic dianhydride (BTDA) and 4, 4′-(1,4-Phenylenediisopropylidene) bisaniline(PDBA) were purchased from Sigma-Aldrich.1-Butyl-3-methylimidazolium chloride was synthesized according to a procedure reported in the literature [40]. Meta-cresol, triethylamine (TEA), triphenylphosphite (TPP), benzoic acid (BA), glacial acetic acid, phosphoric acid (85 %) and (S)-(+)-Histidine hydrochloride monohydrate were purchased from Merck. All other materials were used as received.

Monomer and polymers synthesis

Synthesis of diacid-diimide monomer bearing imidazole groups

Here, 2.51 g (12 mmol) of (S)-(+)-Histidine hydrochloride monohydrate and 1.61 g (5 mmol) of 3,3′,4,4′-Benzophenone tetracarboxylic dianhydride (BTDA) were placed into a 100 mL double-necked round-bottomed flask, equipped with a nitrogen inlet and outlet and a reflux condenser. Then, 60 ml of glacial acetic acid was added to the flask and the mixture was magnetically stirred at room temperature under nitrogen

flow until the solid was completely dissolved. The reaction solution was refluxed at 120 °C for 24 h; after that, the solvent was removed under reduced pressure, the residue was added to 100 ml of distilled water and the pH of the solution was adjusted to neutral by the drop-wise addition of 0.5 M NaOH. A pale yellowish precipitate formed immediately, which was filtered and washed with distilled water before being dried at room temperature.

Melting point (mp): 202–204 °C, [α_D ^{25}]: 95.8° (0.050 g in 10 mL DMF); IR (KB): 3300–2500 (O-H), 1707 (C=O imide), 1774 (C=O), 1597 (C=N), 1374 (C-N), 1097 (C-O), 838 (Ar), 728 (Ar), cm^{-1}; Elem. Anal. calcd. for $C_{29}H_{20}N_6O_9$ (596.5): C, 58.39 %; H, 3.38 %; N, 14.09 %. Found: C, 58.28 %; H, 3.20 %; N, 13.77 %. EI-MS: 596 (0.3, M+), 392 (2.8), 377 (2.6), 283 (1.2), 237 (40.5), 131 (78.1), 103 (58.2), 83 (52.2), 77 (43.8), 55 (83.5), 43 (92.3), 42 (80.5), 41 (100).

The synthesis route of the monomer is shown in Scheme 1.

Synthesis of poly(amide-imide) (PAI)

Here, 1.6 g (2.81 mmol) of synthesized diacid-diimide and 1.16 g (3.37 mmol) of 4,4′-(1,4-Phenylenediisopropylidene) bisaniline (PDBA) were placed in a 50 ml double-necked round-bottomed flask, containing 7 g ionic liquid (1-Butyl-3-methylimidazolium chloride) and 1.5 ml triphenylphosphite. A reflux system with a magnetic stirrer was set up and the reaction was equipped with a nitrogen inlet and outlet. The mixture was stirred at 60 °C for 1 h and then refluxed with constant stirring at 140 °C for 12 h. The resulting brown and viscose solution was cooled to room temperature and poured drop-wise into 500 mL of methanol under constant stirring. The formed precipitate with pale yellow color was filtered off and washed with methanol and distilled water several times. The polymers were dried under vacuum and then placed in an oven at 70 °C in vacuum overnight to remove all residue of the solvent. Scheme 2 shows the synthesis route of the PAI. The molecular weight M_w of the poly(amide-imide) (PAI) was about 2.3×10^4 (M_w/M_n=1.96).

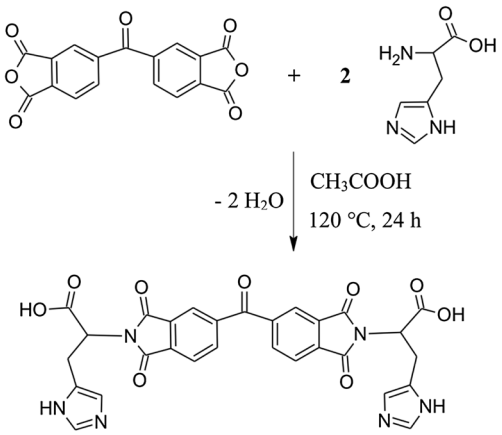

Scheme 1 Synthesis route of diacid-diimide monomer

Synthesis of sulfonated polyimide (SPI)

Sulfonated polyimide was synthesized by reacting sulfonated and non-sulfonated diamines with a six-membered naphthalene base dianhydride through solution imidization. A representative SPI (DSDSA/PDBA/NTDA) with molar ratio of (1/1/2) was prepared as shown in Scheme 3.

Here, 68 ml of m-cresol was added to 2.96 g (8 mmol) of sulfonated diamine, 4,4-diaminostilbene-2,2-disulfonic acid (DSDSA), in a 250 ml double-necked round-bottomed flask with a nitrogen inlet and outlet. A reflux system with a dean-stark trap and a powerful magnetic stirrer was set up. Then, 2.5 ml (17.92 mmol) TEA was added dropwise to the mixture while stirring at room temperature. The mixture was heated at 70 °C until the DSDSA was dissolved (about 1 h), after which the temperature was decreased to 30 °C and 2.76 g (8 mmol) PDBA, 4.3 g (16 mmol) NTDA and 3.90 g of benzoic acid were added individually and subsequently. The mixture then was stirred at 80 °C for 4 h and 180 °C for 24 h. At the end, 50 ml m-cresol was poured into the highly viscose dark brown solution to reduce the viscosity and then the temperature was decreased to 80 °C. The reaction mixture was poured gently into 800 ml of acetone with a mixer and stirred for 1 h. The polymer fibers were filtered and washed with further acetone and dried in vacuum at 120 °C for 24 h. The molecular weight M_w of the sulfonated polyimide (SPI) was about 5.7×10^4 (M_w/M_n=3.2).

Membrane preparation

All membranes were prepared by a solution-casting method. The SPI and SPI/PAI membranes were fabricated by casting a 5%wt solution of pure SPI or SPI/PAI polymer blends in m-cresol on a glass sheet. The homogeneous solutions were filtered and casted at 80 °C and casted membranes were dried at 110 °C for 15 h. The as-cast membranes were separated from glass by immersing in distilled water. After that, the membranes were soaked in methanol for 24 h at room temperature to remove the residual solvent and then treated with 2.0 M HCl at room temperature for 48 h and at 50 °C for 12 h for exchanging the Et_3N groups to the H^+ ions. The proton-exchanged membranes were thoroughly washed with distilled water and then dried in a vacuum oven at 120 °C for 12 h. Five membrane samples prepared by this method consisted of a pure SPI sample and four blend membranes, with 5, 10, 15 and 20 %(*w/w*) ratios of PAI to SPI. The blend membranes were named SPI/PAI-5 %, SPI/PAI-10 %, SPI/PAI-15 % and SPI/PAI-20 %, respectively. All of the mentioned membranes are shown in Fig. 1.

Scheme 2 Synthesis route of poly(amid-imide)

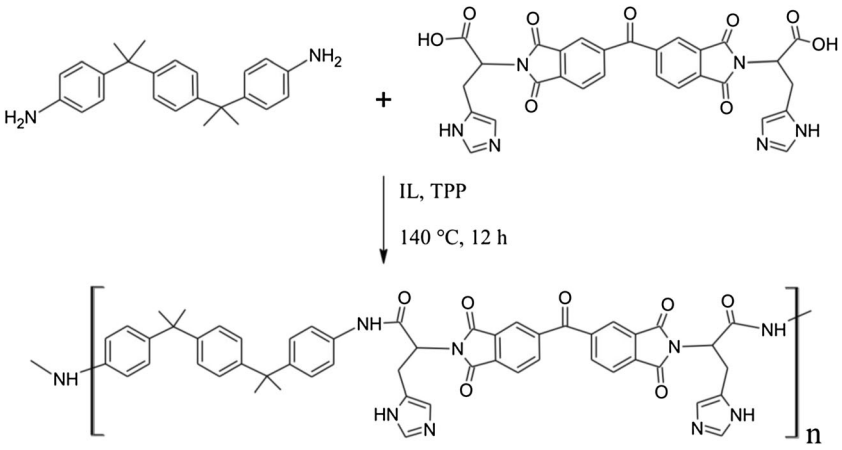

Preparation of phosphoric acid doped (SPI/PAI) membranes

Homopolymeric PAI with imidazole groups was blended with SPI, in order to be doped with phosphoric acid. Phosphoric acid molecules have the potential to form an acid-base complex with imidazole groups of PAI, existing in the blend membranes. The vacuum dried SPI/PAI membranes in acid form were immersed in phosphoric acid 85 % at 60 °C for 24 h. The result PA doped (SPI/PAI)membranes were soaked in distilled water while stirring for 10 min to remove the extra phosphoric acid, and then the membranes were dried with paper towels.

Membrane characterization

Instrumentation

The synthesized monomer and polymer structures were confirmed by ^{1}H NMR and ^{13}C NMR spectra and Fourier Transform attenuated total reflectance (FT-ATR) spectroscopy. The ^{1}H NMR and ^{13}C NMR spectra were measured on a Bruker (400 MHz) spectrometer using DMSO-d_6 as solvent and tetramethylsilane (TMS) as an internal standard. The ATR-FTIR spectra (600–4000 cm^{-1}) were recorded with a Bruker Equinox 55 FT-IR Spectrometer. Thermogravimetric analysis (TGA) was performed on a Rheometric Scientific STA 1500. The samples were heated from room temperature to 800 °C under Argon atmosphere at a scanning rate of 10 °C/min. Tensile measurements were performed with a mechanical tester Instron-5566 instrument at a speed of 5 mm/min. Samples were dried at ambient conditions for 1 day and tested at room temperature and ambient humidity (about 25 °C and 40 % relative humidity). The sample dimensions were 9×50 mm with an average thickness of 60 μm, so that 15 mm of each sample was put in the pulling jaws up and downwards and a the remaining 20 mm of the membranes was pulled between the jaws with at a constant speed. The membrane morphologies were investigated by a Seron AIS2300 scanning electron microscope, while the surface and cross-section of membrane samples were coated with a nanometric layer of sputtered gold. The measurements of proton conductivity, σ (mS.cm^{-1}), of the membrane samples were performed using an AC impedance spectroscopy by an Autolab PGSTAT302N Potentiostat-Galvanostat Impedance Analyzer over the frequency of 0.01 Hz–100 kHz and 50 mV Amplitude. Waters 410 Gel permeation chromatography (GPC) instrument fitted with an RI detector was used to determine the molecular weights of the sulfonated polyimide and Poly(amide-imide)

Scheme 3 Synthesis route of sulfonated polyimide (SPI) copolymer

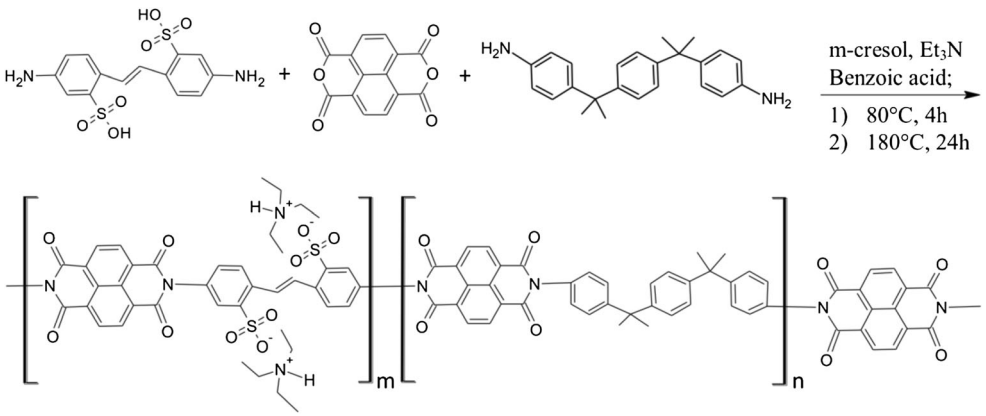

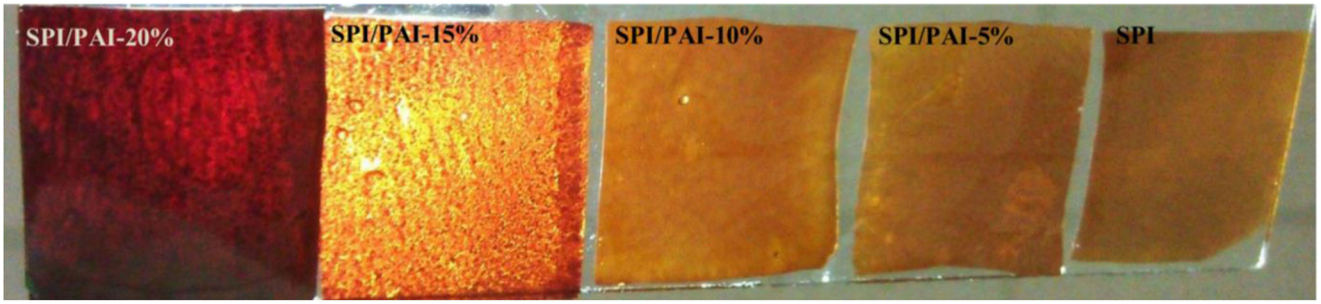

Fig. 1 Top view of the pure SPI and SPI/PAI blend membranes

bearing imidazole groups. N,N-dimethylformamide (DMF) was used as the eluent and polystyrene was used as the standard. Mass spectrum was recorded on an Agilent Technology (HP) MS Model: 5973 Network Mass Selective Detector, instrument by Electron Impact (EI) Ionization mode with an ionization voltage of 70 eV. Elemental analyses (C, H, N) were performed with a Heraeus CHN O-Rapid analyzer.

Water uptake

The water sorption values of the membranes were determined at 30 °C. The membranes were vacuum-dried at 120 °C for 12 h, weighed and immersed in distilled water for 24 h. The wet membranes were wiped with tissue paper and quickly weighed. The water uptake (WU) of the membranes was calculated in weight percent by Eq. (1):

$$WU(\%)\frac{W_{wet}\cdot W_{dry}}{W_{dry}} \times 100 \quad (1)$$

Where W_{wet} and W_{dry} are the weights of water-swollen and dry membranes, respectively. Water uptakes of the corresponding phosphoric acid doped membranes also were measured by the same procedure.

Ion exchange capacity

Ion exchange capacity (IEC) of the pure SPI and blend SPI/PAI membranes, before and after doping with phosphoric acid, was calculated by the titration method. The membranes in the H^+ form were immersed in a 1 N NaCl solution at 50 °C for 48 h to exchange the H^+ ions of the membrane with Na^+ ions in the solution. Then, the released H^+ ions within the solution were titrated with 0.02 N NaOH using phenolphthalein as an indicator, while the membrane was still present in the solution during titration. The IEC was calculated by the following formula using Eq. (2):

$$IEC = \frac{M \times V_{NaOH}}{W_{dry}} \quad (2)$$

Where IEC is the ion exchange capacity, expressed in meq.g^{-1}, M is the molarity, V is the volume of titrated NaOH and W_{dry} is the weight of dried membranes in vacuum oven in 120 °C for 12 h, before immersing in NaCl solution.

Proton conductivity

Each sample was cut into sections (1.2×2 cm) prior to being mounted between two platinum electrodes on the cell. The membranes were sandwiched between two plates of Pt electrodes (0.8×1.6 cm) and the electrodes were set in a Teflon cell. The Teflon cell was packed between two aluminum plates with a thickness of 1.5 cm, while two controllable heating elements were set inside the aluminum plates for creating various temperature conditions inside the Teflon cell. The membranes were placed in contact with the air through the gaps placed in the Teflon cell and aluminum plates. Before the test, the membranes were soaked in water for 24 h and then the conductivity measurements were performed at ambient humidity (about 40 % RH). The proton conductivity, σ, of the membrane was calculated from Eq. (3):

$$\sigma = \frac{l}{R \times A} \quad (3)$$

Where l is the distance (cm) between the Pt electrodes, which here is the same as the membrane thickness. R is the resistance value measured with Autolab impedance analyzer and A is the surface area (cm^2) required for a proton to penetrate the membrane that equals with the Pt plates surface area. The impedance of each sample was measured three times to ensure good data reproducibility.

Results and discussion

Synthesis and characterization of diacid-diimide monomer bearing imidazole groups

As outlined in Scheme 1, diacid-diimide was synthesized by the condensation of one equiv. of 3,3′,4,4′-Benzophenone tetracarboxylic dianhydride (BTDA) with two equiv. of (S)-(+)-Histidine hydrochloride monohydrate in acetic acid as a solvent. After

dissolving the materials, diacid-diimide was synthesized via imidization reaction between the amine and dianhydride, under refluxing conditions in a nitrogen atmosphere. Monomer structure was determined and confirmed by ^{1}H NMR, ^{13}C NMR and FT-ATR techniques. The ^{1}H NMR spectrum of diacid-diimide (Fig. 2) showed a peak at 4.89 ppm that was assigned to the proton of the chiral center.

The peaks of aromatic protons are shown at 6.91–8.21 ppm. The ^{13}C NMR spectrum of this compound properly matched with ^{1}H NMR spectrum. A peak at 53.17 ppm was attributed to the chiral center carbons and the highest chemical shift at about 193 ppm was attributed to the carbonyl group of the centric ketone. The mentioned peaks and the peaks of aromatic region are shown in Fig. 3.

The FT-ATR spectrum of the monomer (Fig. 4a) showed a peak at 1774 cm^{-1} that was ascribed to C=O stretching of centric ketone and the sharp and intense peak at 1707 cm^{-1} was assigned to acidic and imidic carbonyls.

The peak at 1597 cm^{-1} showed the C=N bond of imidazole ring and the imidic C−N bond was showed at 1374 cm^{1}. Also, 728 and 838 cm^{-1} peaks are attributed to the bending of aromatic rings and the peak of the C−O bond of carboxylic acid was shown at 1097 cm^{-1}.

Polymer synthesis

Synthesis and characterization of poly(amide-imide) (PAI)

A poly(amide-imide) with imidazole groups on the polymer chain was synthesized successfully by direct polycondensation of one equiv. of synthesized diacid-diimide monomer with one equiv. of 4,4′-(1,4-Phenylenediisopropylidene) bisaniline (PDBA), in ionic liquid (1-Butyl-3-methylimidazolium chloride) as a solvent and catalyst in the presence of triphenylphosphite (TPP) as an activating agent. Polymer structure was characterized with ^{1}H NMR and FT-ATR spectrum. The ^{1}H NMR spectrum showed a doublet peak at 1.51 and 1.55 ppm that was attributed to the aliphatic hydrogen of methyl groups and a singlet peak at 10.27 ppm, assigned to the amidic proton. The weak peak at 4.9 ppm was assigned to the chiral center protons. The other peaks that belong to the aromatic region protons appeared between 6.42 and 8.45 ppm (Fig. 5).

The ATR-IR spectrum showed absorption bands at 1774 cm^{-1}(C=O of centric ketone), 1710 cm^{-1}(acidic and imidic C=O), 1609 cm^{-1}(C=N of imidazole ring), 1373 cm^{-1}(imidic C–N), 1512 cm^{-1} (aromatic C=C)

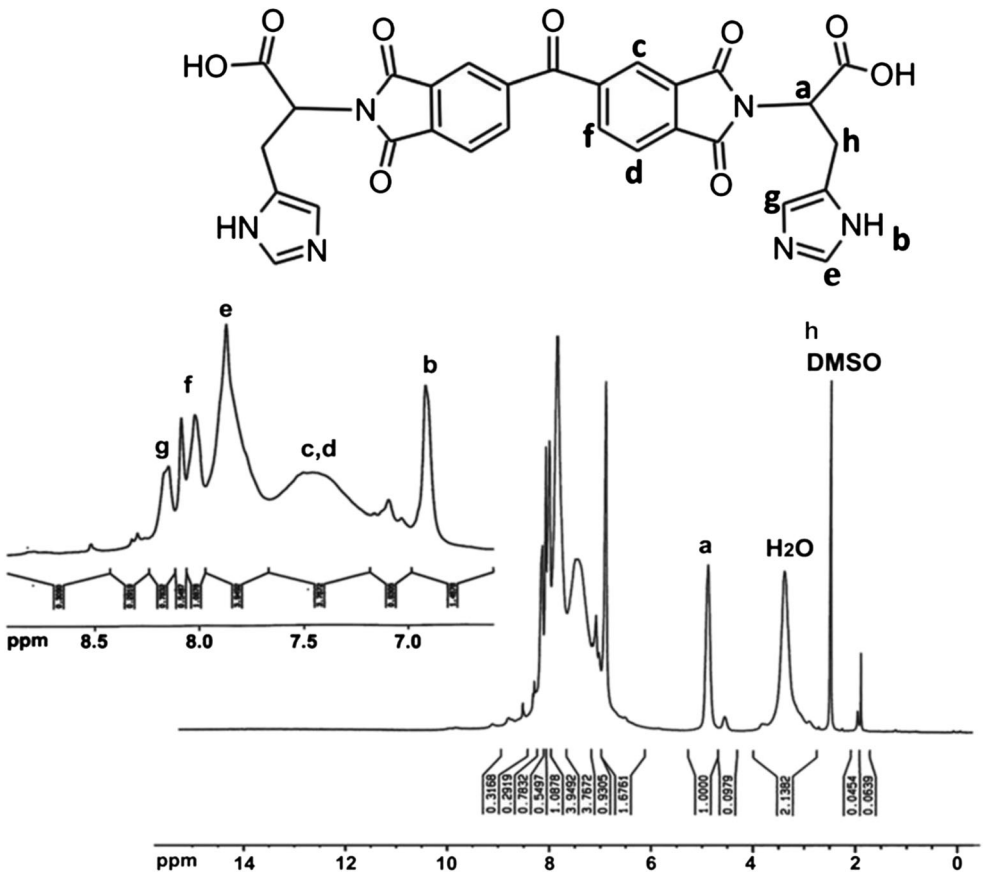

Fig. 2 ^{1}H NMR spectra of diacid-diimide monomer

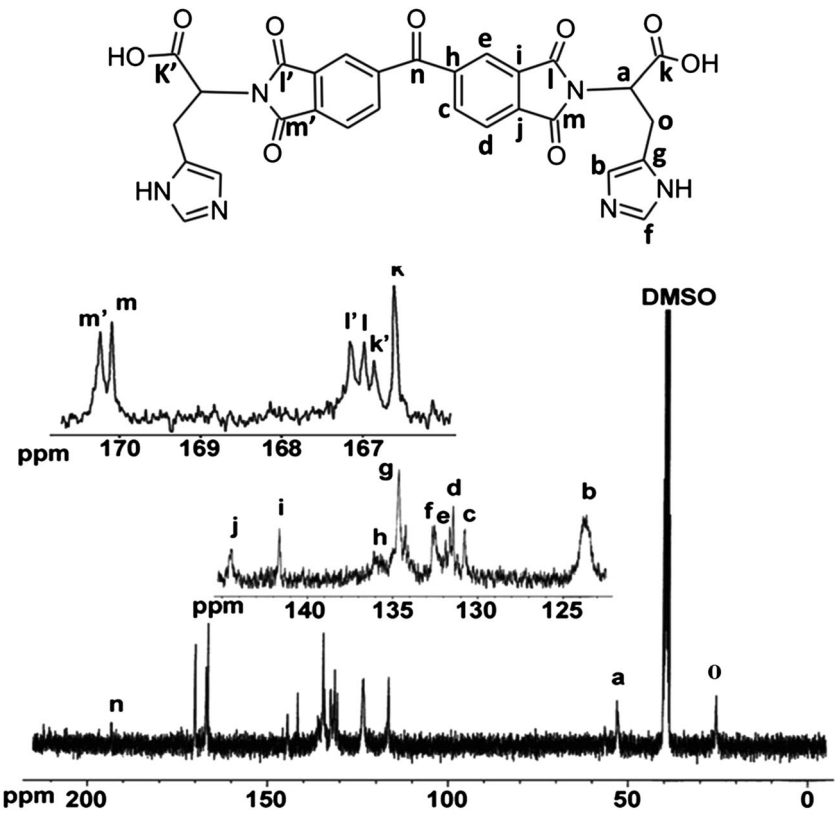

Fig. 3 ^{13}C NMR spectra of diacid-diimide monomer

and 830 cm^{-1}, 744 cm^{-1} (C–H bending of aromatic rings) (Fig. 4b).

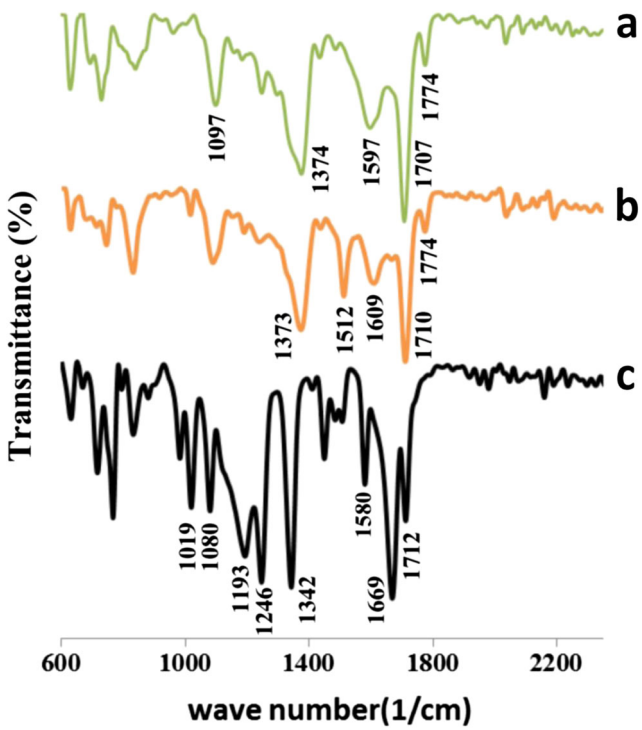

Fig. 4 FT-ATR spectra of diacid-diimide monomer (**a**), poly(amide-imide) (PAI) (**b**) and sulfonated polyimide (SPI) (**c**)

Synthesis and characterization of sulfonated polyimide (SPI)

Sulfonated polyimide (SPI) was synthesized via a solution imidization reaction. The ^{1}H NMR spectrum of SPI showed a singlet and sharp peak at 1.73 ppm that was attributed to the hydrogen of methyl groups. Another singlet and sharp peak at 4.26 ppm was ascribed to the protons of aliphatic double bonds in the sulfonated monomer (DSDSA) structure. The peaks of aromatic region hydrogen appeared in the range of 7.29-8.74 ppm, as shown in Fig. 6.

The ATR-IR spectrum of SPI (Fig. 4c) showed strong absorption bands around 1712 cm^{-1} ($_{sym}$ C=O), 1669 cm^{-1} ($_{asym}$ C=O) and 1342 cm^{-1} (C–N imide), were assigned to the naphthalimide absorption bands. The broad bands at 1019, 1080 and 1193 $cm^{-}1$ were attributed to the symmetric and asymmetric stretching vibrations of the sulfonic acid groups [41, 42]. Aromatic rings bending peaks were appeared around 766 and 829 cm^{-1}.

Membranes morphology

The surface and cross-section morphology of the membranes in acid form was investigated using scanning electron microscopy (SEM) and the images are depicted in Fig. 7.

The cross-sectional pieces of the membrane were prepared by immersing and then fracturing the membranes

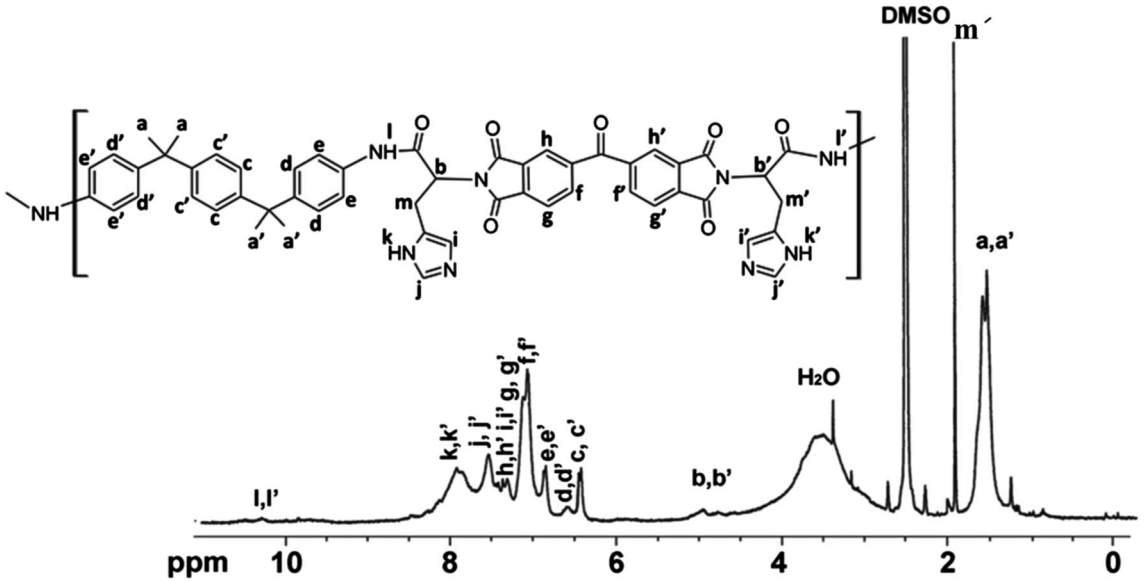

Fig. 5 ^{1}H NMR spectra of poly (amide-imide) (PAI)

annealed in liquid nitrogen. The SEM images showed that the membranes have a dense surface without any pores. Pure SPI membrane showed a homogeneous and dense structure with good uniformity. The PA-doped blend membranes including SPI/PAI-5 % and SPI/PAI-10 % also had good uniformity and good dispersion with a small amounts of unresolved particles in the membrane surface, showing that the PAI is distributed uniformly in the films, but more small sediments sticking together on one side of SPI/PAI-15 % and SPI/PAI-20 % membranes can be detected from the images. It was found that increasing the PAI percentage and doping with phosphoric acid in blend membranes could change the membrane morphology and also the excess amounts of PAI would increase the micrometer-sized agglomerated polymeric particles in the membrane matrix that could decrease the uniformity of the membranes overall. The morphology of membranes could effectively influence membrane properties such as mechanical stability, water uptake and conductivity.

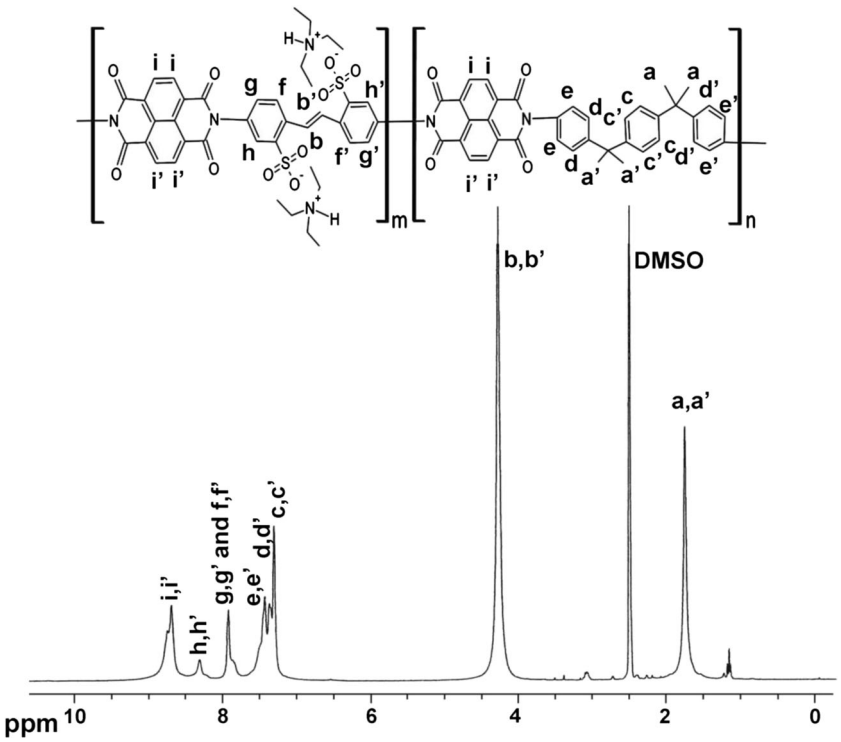

Fig. 6 ^{1}H NMR spectra of sulfonated polyimide (SPI)

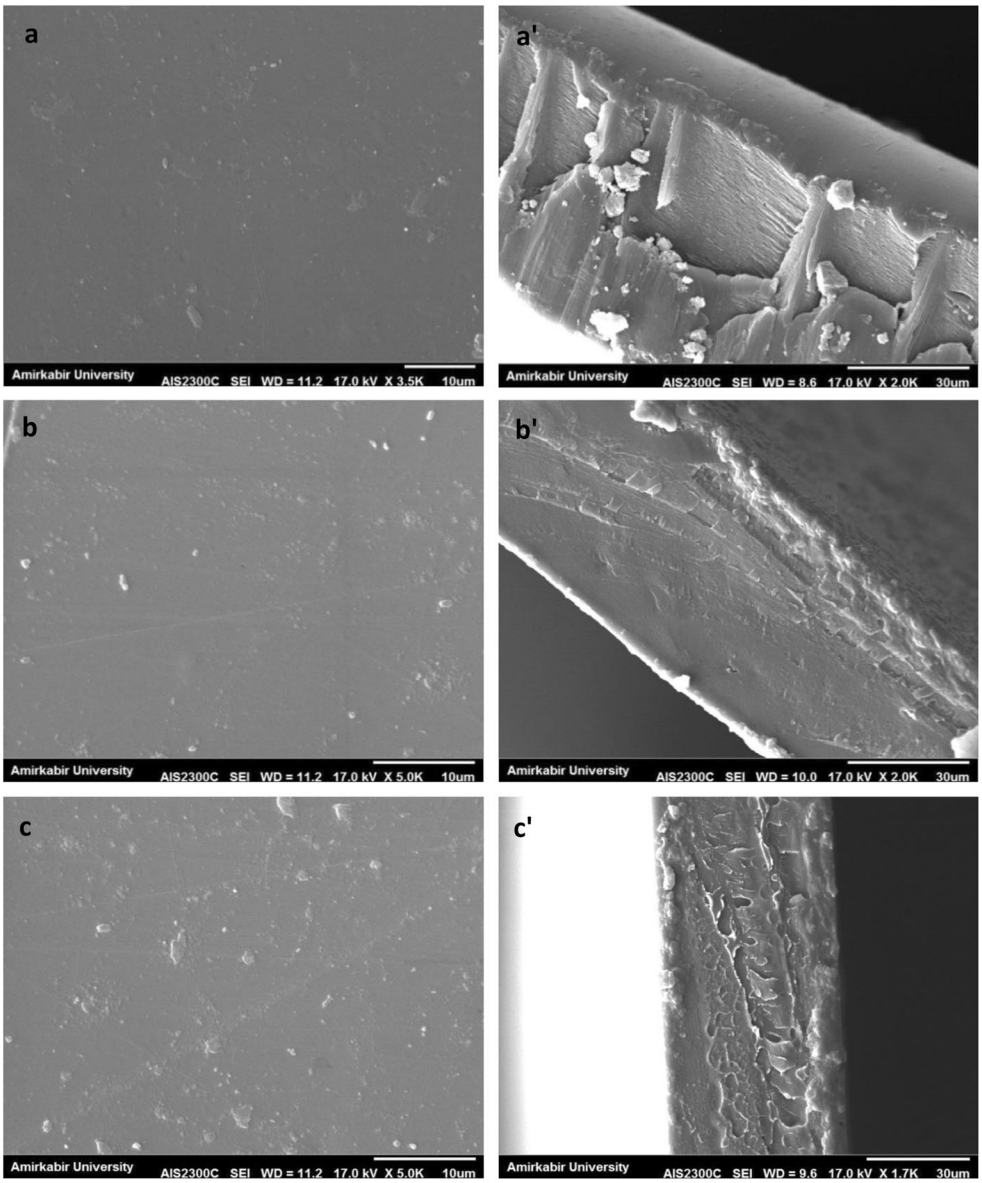

Fig. 7 Surface (*left*) and cross-sectional (*right*) view of SEM images for pure SPI (a, a′) - SPI/PAI-5 % (b, b′) - SPI/PAI-10 % (c, c′) - SPI/PAI-15 % (d, d′) - SPI/PAI-20 % (e, e′)

Thermal stability

Thermal stability of the membranes in protonated form, consisting of pure SPI and phosphoric acid doped blends (SPI/PAI-5 %, SPI/PAI-10 %, SPI/PAI-15 % and SPI/PAI-20 %), and also the thermal stability of pure PAI powder, were investigated by TGA in an argon atmosphere, at a scanning rate of 10 °C/min; the results are shown in Fig. 8.

All of the samples showed a typical three-step degradation pattern. The first step of degradation in pure SPI at about 120 °C is due to the loss of water molecules absorbed by the highly hygroscopic SO_3H groups. The second weight loss that started around 290 °C was assigned to the degradation of SO_3H groups. Finally the substantial weight loss at about 530 °C was attributed to the cleavage of the main polymer chain of SPI [43, 44]. The SPI copolymer membrane still had about 80 % weight remaining at 500 °C that shows the considerable thermal stability of the SPI copolymer. The TGA curve of pure PAI also exhibited a three-step decomposition pattern. The first weight loss at about 100 °C is due to the loss of water absorbed from atmospheric humidity upon storing and preparing the PAI sample for the TGA measurements, whereas the second one observed at about 250 °C, could be attributed to the degradation of imidazole rings, existing on the polymer chain. The third weight loss which began from about 410 °C corresponds to the cleavage of the PAI backbone. As seen from the curves,

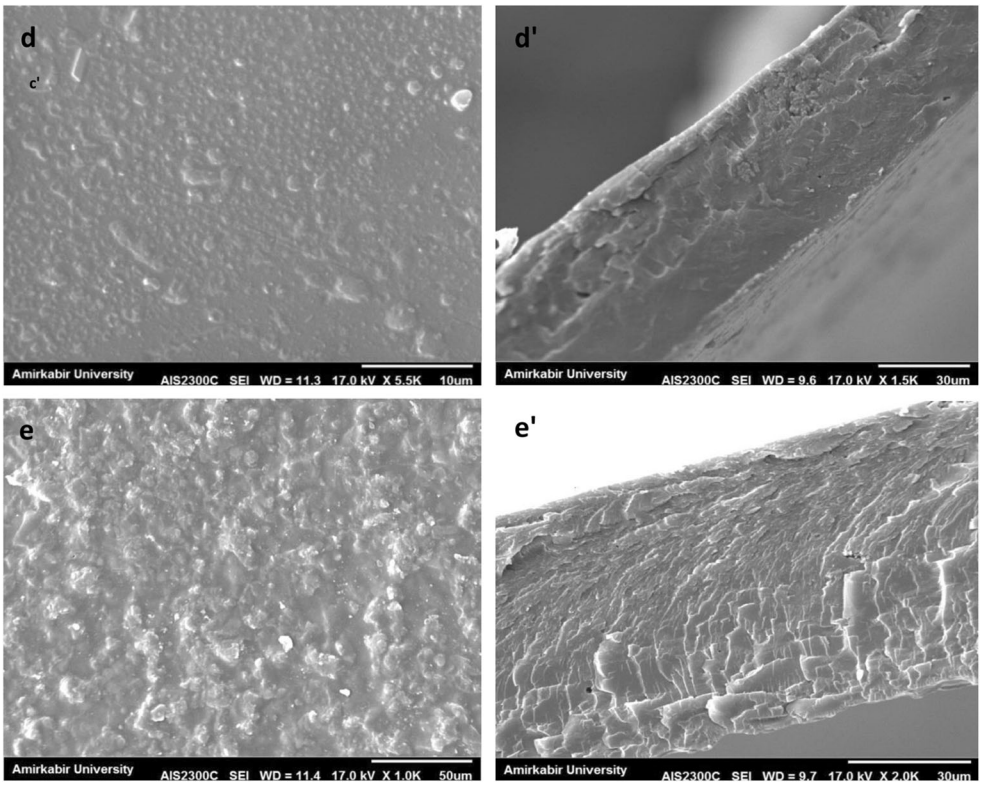

Fig. 7 (continued)

all of the samples had a relatively high thermal stability. Pure SPI membrane had the highest decomposition temperature while the decomposition temperature of pure PAI was lower than the other samples. The remaining samples were placed between these two levels of stability. According to the curves, as the amounts of PAI increased in the blend membranes, the last degradation temperature somewhat decreased because of the lower thermal stability of PAI in compared with pure SPI, but their weight residues a little increased before occurring the last decomposition. Generally, before about 300 °C, the pure PAI and SPI showed the lowest and highest weight losses among the samples respectively, and the weight loss values totally decreased in blend membranes compared to the pure SPI. This could be attributed to the intermolecular interactions between the functional groups of PAI and SPI. However, at the temperatures between about 500–720 °C, pure SPI showed the highest thermal stability and as the PAI ratios increased, the weight losses increased in blend samples. Table 1 shows the weight losses

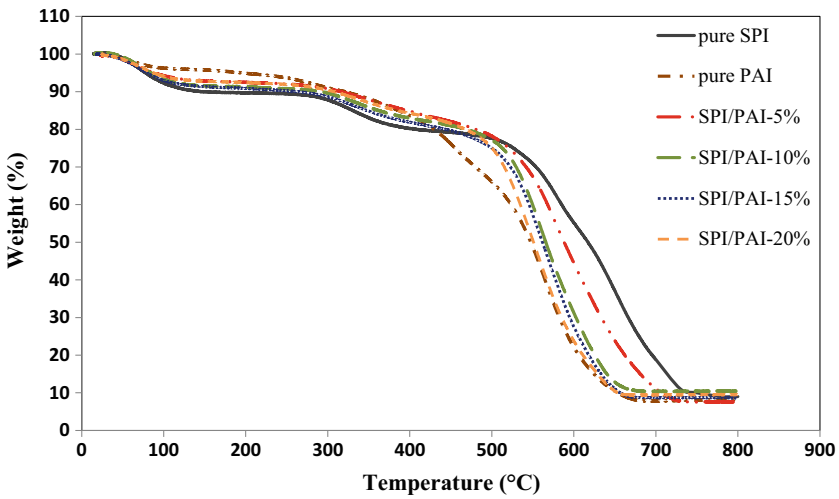

Fig. 8 Thermogravimetric analysis (TGA) curves of the pure SPI, pure PAI and SPI/PAI blend membranes, in Argon atmosphere and 10 °C/min heating rate

Table 1 Thermal stability data of PAI, SPI and blend membranes

Samples	2nd weight loss start up (°C)	3rd weight loss start up (°C)	Weight loss (%) until			
			200 °C	400 °C	600 °C	800 °C
PAI	247	410	5.1	16.4	77.9	91.8
SPI	287	532	10.3	19.9	44.8	90.9
SPI/PAI-5 %	284	521	7.6	15.3	45.7	92.4
SPI/PAI-10 %	285	517	8.7	17.1	68.9	89.6
SPI/PAI-15 %	282	511	9.2	18.1	72.5	91.4
SPI/PAI-20 %	283	502	7.7	15.8	76.4	90.5

start up temperatures and also weight loss amounts of the samples at different temperatures.

Mechanical properties

The mechanical stabilities of membranes (in acid form) were evaluated by means of tensile strength at ambient state; the resulting strain-stress curves are indicated in Fig. 9 and Table 2.

All of the films were strong and flexible with a thickness of 56–63 micrometers. The films showed different tensile strengths in the ranges of 59.4–91.3 Mpa, Young-modulus of 1.26–2.41 Gpa, and Elongation at break of 5.3–16.6 %, illustrating that they have reasonably high values of mechanical properties. As shown by the previous works, phosphoric acid could influence the mechanical properties of the membrane with respect to the types of polymer and the amounts of doped PA. The phosphoric acid may increase the elongation at break due to the increasing space between the polymer chains; therefore, it can also weaken the membrane strength by reducing the intermolecular forces. On the other hand, it can make the membranes more brittle at higher doping levels of PA [45–47]. The pure SPI showed a tensile stress of 74.2 Mpa, Young-modulus of 1.80 Gpa and elongation at break of 9.2 %. According to the data, adding 5 and 10 W% of PAI into the SPI membranes increased the elongation at break of the samples, but introducing more amounts of PAI reduced the elongation at break for samples with 15 and 20 w% of PAI in PA-doped blend membranes. Moreover, the maximum tensile stress of the films reduced in samples with 5, 10 and 15 % of PAI compared to pure SPI, while the young modulus enhanced as the PAI ratios increased in blend samples. The sample SPI/PAI-20 % showed an increase in the maximum tensile stress and Young-modulus and a reduction of elongation at break, which implies its greater stiffness and lower flexibility compared to the pure SPI and other membranes.

Water uptake

The hydration state of a membrane has an important effect on the proton conductivity [48]. Acid groups capable of liberating H^+ ions for the generation of H_3O^+ through dissociation in water have an important role in the proton conductivity. H_2O molecules cause the

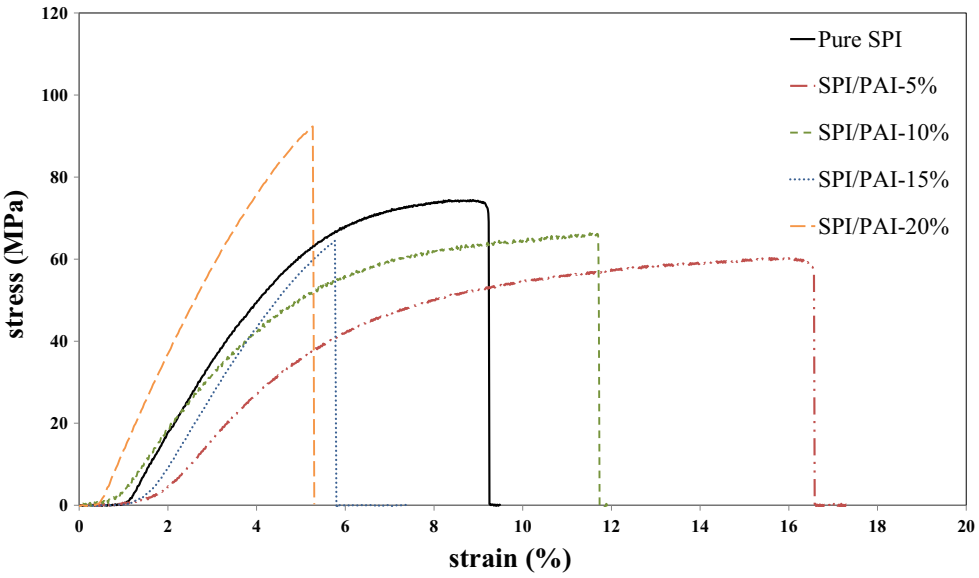

Fig. 9 Stress-strain curves of SPI and phosphoric acid doped SPI/PAI membranes. Samples were dried at ambient conditions for 1 day and tested at 25 °C and 40 % RH

Table 2 Mechanical properties of the membranes in protonated form

Membranes	Thickness (μm)	Tensile strength (MPa)	Young's modulus (GPa)	Elongation at break (%)
SPI	63	74.2	1.80	9.2
SPI/PAI-5 %	58	59.4	1.26	16.6
SPI/PAI-10 %	56	65.8	1.53	11.7
SPI/PAI-15 %	58	63.5	1.78	5.8
SPI/PAI-20 %	62	91.3	2.41	5.3

dissociation of acid functional groups and also help with proton transport in the membrane. However, the excessive and unnecessary amounts of water sorption will reduce the mechanical stability of the membranes and can limit their practical use as polymer electrolyte membranes. So the optimal values of water uptake have a key role in PEM membranes. The water uptake data of the pure SPI and also SPI/PAI membranes before and after doping with phosphoric acid are given in Table 3.

The pure SPI showed a water uptake of 34.13 %. As the weight percent of PAI increases in SPI/PAI samples, the number of imidazole groups increase and the amounts of SPI and SO_3H groups decrease subsequently. SO_3H groups have more important role in water sorption compared to imidazole groups; therefore, as Table 3 shows, the water uptakes of SPI/PAI membranes without PA doping, decrease with the increment of PAI ratios, accompanied with the reduction of SPI ratios. Moreover, the PA doped membranes showed different results. SPI/PAI-10 % displayed the maximum water uptake (47.19) among the samples. Water sorption in pure SPI, SPI/PAI-5 % and SPI/PAI-10 % samples increased, and decreased in SPI/PAI-15 % and SPI/PAI-20 % samples. Blending of SPI with PAI, on the one hand, decreases the ratio of SPI and also the number of SO_3H groups and would decrease the water sorption of the film; on the other hand, doping of blend membranes with phosphoric acid could potentially increase the water sorption of films through the formation of hydrogen bonds between phosphoric acid and water molecules. However, it seems that the W% of PAI in blend membranes has an important role in the water uptake of the membranes. In other words, increasing the percentage of PAI to 10 % can increase the water sorption through the interaction of doped phosphoric acid with H_2O molecules, but further increase of PAI might change the blend membrane morphology and obstruct the water carrier channels of the SPI membrane that leads to the reduction of water uptake in SPI/PAI-15 % and SPI/PAI-20 % samples.

Ion exchange capacity (IEC)

The experimental Ion exchange capacity of the membranes in the protonated form, including pure SPI, non-doped SPI/PAI membranes and phosphoric acid doped SPI/PAI membranes, was determined by titration methods and the resulting IECs calculated from Eq. (2) are given in Table 3. The pure SPI membrane had an IEC of 1.76 meq.g^{-1} and SPI/PAI-10 % showed the highest IEC value among the samples (2.23 meq. g^{-1}). Although all of the PA doped membranes showed higher IECs than pure SPI, the IECs of SPI/PAI-15 % and SPI/PAI-20 % membranes reduced compared to SPI/PAI-10 % and SPI/PAI-5 %. Since the total weight of SPI and PAI are constant in all of the membrane samples, as the PAI percent increases in the membrane, the SPI percent and also the number of SO_3H groups reduces. Increasing the PAI can engage a greater number of phosphoric acid molecules with the membrane, which can raise the IEC; on the other hand, it will reduce the SO_3H groups that will lower the IEC value. Therefore, finding an optimum ratio between them would give more optimal values of IEC. The IEC data almost showed desirable agreement with the water uptake of membranes. It was found that the higher blending amounts of

Table 3 IEC, Water uptake and proton conductivity of the membranes

Samples	IEC (meq. g^{-1})		Water uptake (%)		Proton conductivity, σ, (mS cm^{-1})						
	–	PA doped	–	PA doped	25 °C	40 °C	60 °C	80 °C	100 °C	120 °C	140 °C
SPI	1.76	–	34.13	–	10.9	12.1	14.8	18.7	25.8	29.4	26.7
SPI/PAI-5 %	1.67	1.98	32.57	39.62	14.6	16.0	19.3	25.1	32.5	45.3	47.4
SPI/PAI-10 %	1.57	2.23	31.12	47.19	17.8	19.6	24.5	34.1	48.4	63.5	69.7
SPI/PAI-15 %	1.43	1.82	25.89	29.04	9.6	10.8	12.7	15.9	24.5	28.9	29.7
SPI/PAI-20 %	1.31	1.78	24.40	27.16	7.2	7.8	8.8	11.6	18.5	19.8	20.4

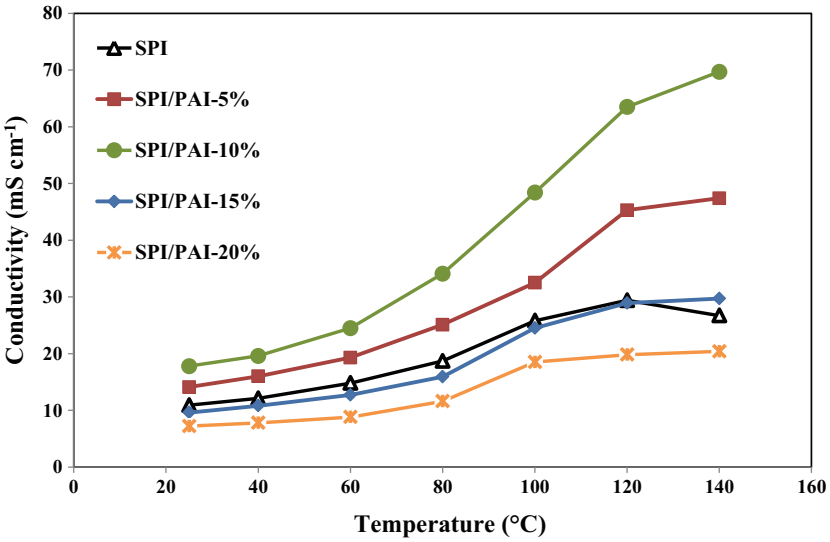

Fig. 10 Proton conductivities of the pure SPI and phosphoric acid doped SPI/PAI membranes at 40 % RH and different temperature conditions

PAI more than 10 % could relatively reduce the IEC and water uptake of the phosphoric acid doped SPI/PAI membranes.

Proton conductivity

Having proper proton conductivity is one of the most important features of a polymer electrolyte membrane. The proton conductivity measurements of the membranes in their acid form were evaluated by an electrochemical impedance spectroscopy technique, through the measurement of membrane resistance via an Autolab impedance analyzer and a proton conductivity cell. Resistance and proton conductivity of the pure SPI and phosphoric acid doped SPI/PAI membranes were measured at ambient humidity (about 40 % RH) and a range of temperatures. The membrane resistance was obtained from Nyquist diagrams and their corresponding proton conductivities achieved from Eq. (3) are given in Table 3. Temperature dependence of the proton conductivities of the membranes are also summarized in Fig. 10.

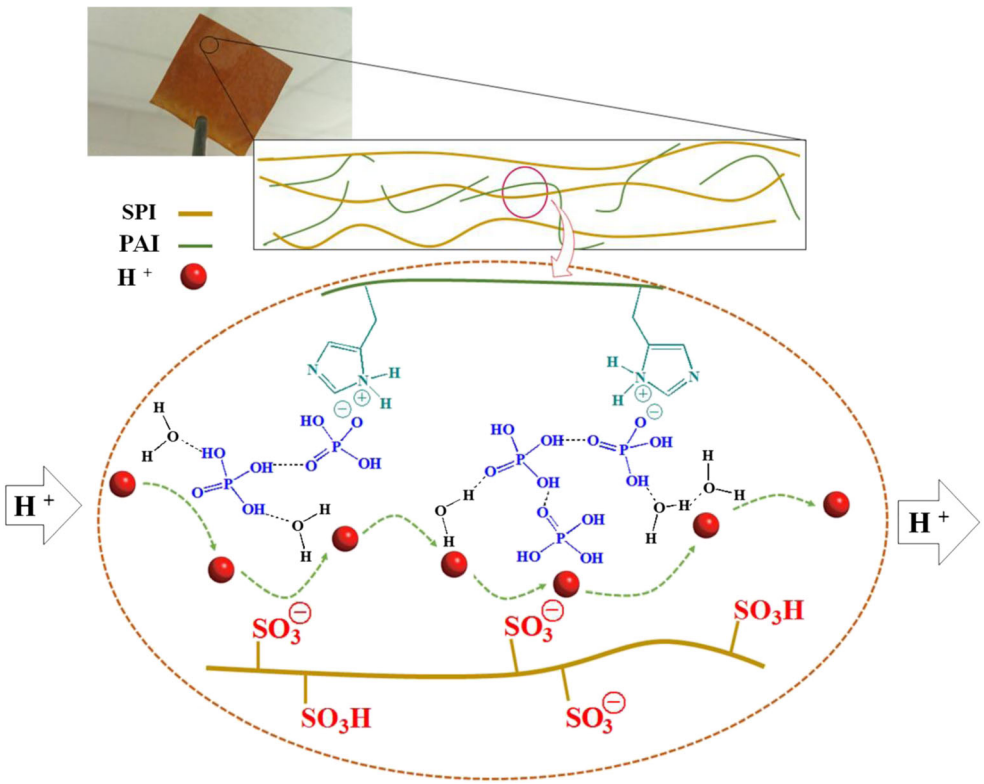

Scheme 4 Schematic representation of proton transfer mechanism in SPI/PAI membrane through the interactions between imidazole Ring, phosphoric acid, sulfonic acid sites and water molecules

Pure SPI membrane with an IEC of 1.76 meq.g^{-1} and water uptake of 34.13 % showed proton conductivities in the range of 10.9 to 29.4 mS cm^{-1}, while phosphoric acid doped membrane SPI/PAI-10 % with an IEC of 2.23 meq.g^{-1} and water uptake of 47.19 % showed the highest proton conductivities in the range of 17.8 to 69.7 mScm^{-1}. As the diagrams show an increase in temperature leads an increase in proton conductivity due to the streamlined diffusion and thermal motion of protons in channels within membranes. The PA-doped samples of SPI/PA-5 % and SPI/PAI-10 % showed a promotion in proton conductivity values to the pure SPI, implying the positive effect of PA molecules on the membranes conductivity, especially at elevated temperatures. Not only could the phosphoric acid molecules help to improve the water sorption of membranes via the formation of hydrogen bonds with water molecules, but it can also compensate for the lack of water in membranes in high temperatures. Scheme 4 illustrates a proposal mechanism for the proton transfer in PAI/SPI blend membranes.

The imidazole rings could strongly interact with PA molecules to form a resisting acid-base complex which its presence can potentially facilitate the hydrogen bonding between H^+ ions, phosphoric acid, water molecules and sulfonic acid sites .This can provide the pathways for higher proton conductivities.

Although the SPI/PA-15 % and SPI/PAI-20 % samples showed higher conductivities in enhanced temperatures due to the presentation of PA molecules in the membrane matrix, and despite having slightly higher IECs than the pure SPI, they showed lower conductivities than it, at all. The proton conductivity mainly depends on IEC, water sorption state and also membrane morphology. It seems that the excess amounts of PAI have negative morphological effects on SPI/PAI-15 % and SPI/PAI-20 % membranes by changing or blocking their proton conducting channel structures, which leads to the water uptake reduction in these samples rather than the pure SPI membrane.

Conclusion

A series of materials were synthesized in order to be used in the fabrication of proton exchange membranes. A diacid-diimide monomer was synthesized by the condensation of 3, 3′,4,4′-Benzophenone tetracarboxylic dianhydride (BTDA) with (S)-(+)-Histidine hydrochloride monohydrate. A PAI bearing imidazole groups was synthesized by direct polycondensation of the diacid-diimide monomer and 4,4′-(1,4-Phenylenediisopropylidene) bisaniline (PDBA). A sulfonated polyimide (SPI) also was synthesized by polymerization of 4, 4-diaminostilbene-2,2-disulfonic acid (DSDSA) and 4,4′-(1, 4-Phenylenediisopropylidene) bisaniline (PDBA) with 1,4,5, 8-Naphthalenetetracarboxylic dianhydride (NTDA). SPI and phosphoric acid doped SPI/PAI membranes with good filmability were made. The membranes had good uniformity according to the SEM images and the stress-stain curves showed that the membranes had proper mechanical stability. The membranes also showed good thermal stability due to the high thermal stability of the SPI presented in the membrane. The coordination of phosphoric acid molecules with the imidazole groups placed in the main chains of the PAI forms a poly ionic liquid salt involved with phosphoric acid and water molecules, which could improve the water uptake, IEC and the proton conductivity values of the phosphoric acid doped SPI/PAI membranes. The phosphoric acid content in the membrane can overcome the problems resulting from a loss of water at higher temperatures. It was found that a suitable content of PAI in phosphoric acid doped SPI/PAI membranes could effectively improve the water uptake, IEC and proton conductivity of them, but excess PAI can negatively affect the water uptake and proton conductivity. The most efficient PAI content was observed in the SPI/PAI-10 % sample with good mechanical and thermal properties and the most appropriate water uptake, IEC and proton conductivity among the samples.

References

1. Zhang H, Shen PK (2012) Chem Rev 112:2780–2832
2. Hickner MA, Ghassemi H, Kim YS, Einsla BR (2004) Chem Rev 104:4587–4612
3. Arslantas A, Sinirlioglu D, Eren F, Muftuoglu AE, Bozkurt A (2014) J Polym Res 21:437
4. Wang Y, Chen KS, Mishler J, Cho SC, Adroher XC (2011) Appl Energy 88:981–1007
5. Abu-Saied MA, Fontananova E, Drioli E, Eldin MSM (2013) J Polym Res 20:187
6. Zhang J, Xie Z, Zhang J, Tang Y, Song C (2006) J Power Sources 160:872–891
7. Einsla ML, Kim YS, Hawley M, Lee HS, McGrath JE, Liu B, Guiver MD, Pivovar BS (2008) Chem Mater 20:5636–5642
8. Bose S, Kuila T, Nguyen TXH, Kim NH, Lau KT, Lee JH (2011) Prog Polym Sci 36:813–843
9. Ma L, Xu J, Han S, Yang M, Wang Z, Ni H, Gui Y (2014) J Polym Res 21:1–10
10. Chandan A, Hattenberger M, El-Kharouf A, Du S, Dhir A, Self V, Pollet BG, Ingram A, Bujalski W (2013) J Power Sources 231:264–278
11. Yuan S, Guo X, Aili D, Pan C, Li Q, Fang J (2014) J Membr Sci 454:351–358
12. Xu JM, Cheng HL, Ma L, Han HL, Huang YS, Wang Z (2014) J Polym Res 21:423
13. He R, Li Q, Xiao G, Bjerrum NJ (2003) J Membr Sci 226:169–184
14. Seel DC, Benicewicz BC (2012) J Membr Sci 405:57–67
15. Mader JA, Benicewicz BC (2010) Macromolecules 43:6706–6715
16. Lee KH, Lee SY, Shin DW, Wang C, Ahn SH, Lee KJ, Guiver MD, Lee YM (2014) Polymer 55:1317–1326
17. Asano N, Aoki M, Suzuki S, Miyatake K, Uchida H, Watanabe M (2006) J Am Chem Soc 128:1762–1769

18. Hu Z, Yin Y, Kita H, Okamoto KI, Suto Y, Wang H, Kawasato H (2007) Polymer 48:1962–1971
19. Yin Y, Yamada O, Tanaka K, Okamoto K, Liu S, Ye H, Zhou Y, Zhao J, Yanai H, Sato T (2006) Polym J 38:197–219
20. Lee CH, Park CH, Lee YM (2008) J Membr Sci 313:199–206
21. Einsla BR, Kim YS, Hickner MA, Hong YT, Hill ML, Pivovar BS, McGrath JE (2005) J Membr Sci 255:141–148
22. Liaw DJ, Wang KL, Huang YC, Lee KR, Lai JY, Ha CS (2012) Prog Polym Sci 37:907–974
23. Akbarian-Feizi L, Mehdipour-Ataei S, Yeganeh H (2010) Int J Hydrog Energy 35:9385–9397
24. Jiang G, Qiao J, Hong F (2012) Int J Hydrog Energy 37:9182–9192
25. Seo DW, Lim YD, Lee SH, Jeong IS, Kim DI, Lee JH, Kim WG (2012) Int J Hydrog Energy 37:6140–6147
26. Sinirlioglu D, Muftuoglu AE, Bozkurt A (2013) J Polym Res 20: 242
27. Zhao C, Lin H, Han M, Na H (2010) J Membr Sci 353:10–16
28. Li X, Liu C, Zhang S, Yu G, Jian X (2012) J Membr Sci 423:128–135
29. Lin HL, Hu CR, Lai SW, Yu TL (2012) J Membr Sci 389:399–406
30. Li Q, Rudbeck HC, Chromik A, Jensen JO, Pan C, Steenberg T, Calverley M, Bjerrum N, Kerres J (2010) J Membr Sci 347:260–270
31. Yu S, Benicewicz BC (2009) Macromolecules 42:8640–8648
32. Xu H, Chen K, Guo X, Fang J, Yin (2007) Polymer 48:5556–5564
33. Li Q, Jensen JO, Savinell RF, Bjerrum NJ (2009) Prog Polym Sci 34:449–477
34. Pu HT, Qiao L, Liu QZ, Yang ZL (2005) Eur Polym J 41:2505–2510
35. Pu H, Meyer WH, Wegner G (2002) J Polym Sci B Polym Phys 40: 663–669
36. Pu H, Wang D (2006) Electrochim Acta 51:5612–5617
37. Hazarika M, Jana T (2012) ACS Appl Mater Interfaces 4:5256–5265
38. Wu H, Shen X, Cao Y, Li Z, Jiang Z (2014) J Membr Sci 451:74–84
39. Boaventura M, Ponce M, Brandao L, Mendes A, Nunes S (2010) Int J Hydrog Energy 35:12054–12064
40. Wasserscheid P, Welton T (2008) Ionic liquids in synthesis, vol. 1. Wiley Online Library, Weinheim, Germany
41. Mistri EA, Mohanty AK, Banerjee S (2012) J Membr Sci 411:117–129
42. Zhang F, Li N, Cui Z, Zhang S, Li S (2008) J Membr Sci 314:24–32
43. Li N, Cui Z, Zhang S, Xing W (2007) J Membr Sci 295:148–158
44. Wu S, Qiu Z, Zhang S, Yang X, Yang F, Li Z (2006) Polymer 47: 6993–7000
45. Yang J, Li Q, Jensen JO, Pan C, Cleemann LN, Bjerrum NJ, He R (2012) J Power Sources 205:114–121
46. Schmidt C, Schmidt-Naake G (2007) Macromol Mater Eng 292: 1164–1175
47. He R, Li Q, Bach A, Jensen JO, Bjerrum NJ (2006) J Membr Sci 277:38–45
48. Alberti G, Casciola M, Massinelli L, Bauer B (2001) J Membr Sci 185:73–81